The directional occurrence of the Levantine geomagnetic field anomaly: New data from Cyprus and abrupt directional changes

Elsevier Editorial System(tm) for Earth and Planetary Science Letters

Manuscript Draft

Manuscript Number: EPSL-D-20-00917

Title: Investigation of the directional occurrence of the Levantine geomagnetic field anomaly: New data from Cyprus and abrupt directional changes

Article Type: Letters

Keywords: Secular Variation; Geomagnetic field direction; Levantine anomaly; Cyprus; Middle East

Corresponding Author: Dr. Evdokia Tema, Ph.D

Corresponding Author's Institution: Universita' degli Studi di Torino

First Author: Evdokia Tema, Ph.D

Order of Authors: Evdokia Tema, Ph.D; Ian Hedley; Javier Pavón-Carrasco; Enzo Ferrara; Pamela Gaber; Despo Pilides; Michael Toumazou; Yiannis Violaris; Jennifer Webb; David Frankel

Abstract: We present new directional archaeomagnetic results from five archaeological sites in Cyprus. All studied materials come from in situ baked clay structures such as small hearths and ovens, dated from 2000 BCE to 1400 CE. Magnetic mineralogy experiments indicate the presence of a mineral close to magnetite as the main carrier. The Characteristic Remanent Magnetization (ChRM) was determined by stepwise alternating field demagnetization and the mean archaeomagnetic directions obtained are very well-defined. The ten new directions are added to the scant reference dataset for Cyprus and are used for further considerations together with data from nearby countries. To investigate the directional variations of the geomagnetic field in the Eastern Mediterranean and Middle East, we calculated a palaeosecular variation curve covering the last four millennia, using a critical selection of reference data from Cyprus, Israel, Turkey and Syria.. This curve shows several periods characterized by abrupt directional changes while a maximum change in curvature is clearly observed around 900 BCE. The new curves confirm the hypothesis that during the Levantine Iron Age Anomaly, apart the extreme intensity values, the geomagnetic field was characterized by steep inclinations and important directional change. Other periods of important curvature change are identified and deserve further investigation.

Suggested Reviewers: Avto Gogichaishvili Dr.
Instituto de Geofisica, UNAM, Morelia, Michoacán, MEXICO.
avto@geofisica.unam.mx

Anita Di Chiara Dr.
Scripps, La Jolla, CA, USA
adichiara@ucsd.edu

Lisa Schnepp Dr.
Paleomagnetic Laboratory Gams, Austria
Elisabeth.Schnepp@unileoben.ac.at

Marisa Osete Dr.
Facultad de CC. Físicas, Madrid, Spain
mlosete@fis.ucm.es

Sanja Panovska
GFZ-Potsdam, Germany
panovska@gfz-potsdam.de

Opposed Reviewers:

Torino, 29.06.2020

Dear Editor,

please find attached the electronic version of the manuscript:

" Investigation of the directional occurrence of the Levantine geomagnetic field anomaly: New data from Cyprus and abrupt directional changes"

by

Tema, E., Hedley, I., Pavón-Carrasco, F.J., Ferrara, E., Gaber, P., Pilides, D., Toumazou, M., Violaris, Y., Webb, J., Frankel, D.

that we submit for publication at *Earth and Planetary Science Letters.*

Our paper investigates the important Levantine Iron Age Anomaly (LIAA), presenting new high-quality data from Cyprus and a first directional paleosecular Variation curve for Cyprus and Middle East. Our results show important directional changes during the last four millennia. The maximum curvature change, characterized by fast directional variation, is detected around 900 BCE, showing that apart the extreme intensity values, the geomagnetic field during the LIAA was characterized by steep inclinations and important directional change. The geographical occurrence of the LIAA is also investigated showing that the secular variation trend depicted by data from Israel is also seen in the Cypriot data.

We hope that this contribution is of interest for publication in Earth and Planetary Science Letters.

Yours sincerely

Evdokia Tema

Corresponding author:
Dr. Evdokia TEMA
Dipartimento di Scienze della Terra
Università degli Studi di Torino
Via Valperga Caluso, 35 – 10125, Torino, Italy
E-mail: evdokia.tema@unito.it
Tel. 0039 0116708395
Fax. 0039 0116708398

Highlights

- New directional archaeomagnetic data from Cyprus
- Palaeosecular variation curve for Eastern Mediterranean and Middle East
- Directional curvature changes during the last four millennia
- Insights on the directional occurrence of the Levantine anomaly

Investigation of the directional occurrence of the Levantine geomagnetic field anomaly: New data from Cyprus and abrupt directional changes

Tema, E.[1,2,*], Hedley, I.[3,4], Pavón-Carrasco, F.J.[5,6], Ferrara, E.[7], Gaber, P.[8], Pilides, D.[9], Toumazou, M.[10], Violaris, Y.[9], Webb, J.[11], Frankel, D.[11]

[1]Dipartimento di Scienze della Terra, Università degli Studi di Torino, via Valperga Caluso 35, 10125 Torino, Italy, evdokia.tema@unito.it

[2]Alpine Palaeomagnetic Laboratory, via Luigi Massa 4, 12016 Peveragno, Italy

[3]Earth and Environmental Sciences Section, Université de Genève, Rue des Maraîchers 13, 1205 Genève, Switzerland, ian.hedley@unige.ch

[4]Laboratoire de Paléomagnétisme, Musée de Préhistoire des gorges du Verdon, 04500 Quinson, France

[5]Facultad de CC. Físicas, Dpto. de Física de la Tierra y Astrofísica, Universidad Complutense de Madrid, Avd. Complutense s/n, 28040-Madrid, Spain, fjpavon@ucm.es

[6]Instituto de Geociencias IGEO (CSIC-UCM), c/Doctor Severo Ochoa, 7, Edificio Entrepabellones 7 y 8, Ciudad Universitaria, 28040 Madrid, Spain

[7]Istituto Nazionale di Ricerca Metrologica, Strada delle Cacce 91, 10135 Torino, Italy, e.ferrara@inrim.it

[8]Archaeology Program, Lycoming College, One College Place, Williamsport PA, 17701, USA, gaber@lycoming.edu

[9]Department of Antiquities, 1 Museum Avenue, Nicosia 1097, Cyprus, despo_pilides@hotmail.com, violarisyian@gmail.com

[10]Department of Classics, Davidson College, Davidson, North Carolina 28035, USA, mitoumazou@davidson.edu

[11]Department of Archaeology and History, La Trobe University, Melbourne Campus, Bundoora, 3086, VIC, Australia, jenny.webb@latrobe.edu.au, d.frankel@latrobe.edu.au

[*]Corresponding author at: Dipartimento di Scienze della Terra, Università degli Studi di Torino, via Valperga Caluso 35, 10125 Torino, Italy. Tel. +39 011 6708395, E-mail address: evdokia.tema@unito.it

Abstract

We present new directional archaeomagnetic results from five archaeological sites in Cyprus. All studied materials come from *in situ* baked clay structures such as small hearths and ovens, dated from 2000 BCE to 1400 CE. Magnetic mineralogy experiments indicate the presence of a mineral close to magnetite as the main carrier. The Characteristic Remanent Magnetization (ChRM) was determined by stepwise alternating field demagnetization and the mean archaeomagnetic directions obtained are very well-defined. The ten new directions are added to the scant reference dataset for Cyprus and are used for further considerations together with data from nearby countries. To investigate the directional variations of the geomagnetic field in the Eastern Mediterranean and Middle East, we calculated a palaeosecular variation curve covering the last four millennia, using a critical selection of reference data from Cyprus, Israel, Turkey and Syria.. This curve shows several periods characterized by abrupt directional changes while a maximum change in curvature is clearly observed around 900 BCE. The new curves confirm the hypothesis that during the Levantine Iron Age Anomaly, apart the extreme intensity values, the geomagnetic field was characterized by steep inclinations and important directional change. Other periods of important curvature change are identified and deserve further investigation.

Keywords: Secular Variation; Geomagnetic field direction; Levantine anomaly; Cyprus; Middle East

1. Introduction

The Earth's magnetic field, generated by complex magnetohydrodynamic processes deep in the Earth's liquid outer core, is of vital importance for life on the Earth as it protects our planet from damaging solar radiation, acting as a huge natural shield. Although of a general long-term dipolar nature when averaged over thousands of years, it is known that it continuously varies on shorter time scales and over small geographical areas. Reconstructing and modelling such short-term geomagnetic field changes, known as Secular Variation (SV), is very important for obtaining a valuable insight into the processes and mechanisms responsible for the geomagnetic field's generation, its evolution and its applications to the core (Jackson and Finlay, 2015).

In the last decades, attention has been focused on the study of particular features of the Earth's magnetic field SV characterized by intense and short-lived changes that occur at decadal and centennial time scales. Based on archaeomagnetic data obtained from well dated archaeological artifacts in France, several periods of rapid geomagnetic field change have been identified, characterized by sharp changes in the direction, which coincide with intensity maxima, named *archaeomagnetic jerks* (e.g. Gallet et al., 2003). In several other studies, particularly high field intensity values associated with rapid SV rates have been observed (e.g. Ben-Yosef et al., 2009; Gómez-Paccard et al., 2016; Hervé et al., 2017). Such high intensities are a surprising and particularly interesting feature of the past SV, also known as *geomagnetic intensity spikes*. High intensity spikes have been identified in several geographical areas and during different chronological periods but undoubtedly the most documented so far is that one observed around 1000 BCE in the Levantine area and known as the Levantine Iron Age Anomaly, LIAA (see Shaar et al, 2016 and references therein).

The Levantine Anomaly was reported by Ben-Yosef et al. (2009) and Shaar et al. (2011) who observed high intensities in Middle East around 1000 BCE. Further data from Turkey (Ertepinar et al., 2012) also showed unusually high archaeointensity values. Shaar et al. (2016) carefully revised the available Levantine data suggesting the presence of extreme regional intensities with two spikes (around 11^{th} and 8^{th} centuries BCE). More recently, Shaar et al. (2018) presented a large compilation of archaeomagnetic directions from Israel that cover the last four millennia, showing that the Levantine intensity anomaly is also accompanied by significant directional changes. Indeed, the directions from Israel show high inclination and high declination values during the 9^{th} century BCE, providing more evidence for a regional field anomaly in Middle East during the beginning of the first millennium BCE.

Even though, abrupt variations on the direction and/or the intensity of the Earth's magnetic field are a particularly interesting feature of the geomagnetic field, their origin, geographical occurrence and explanation through core-flow dynamics are still under investigation (e.g. Livermore et al., 2014; Davies and Constable, 2018; Korte and Constable, 2018). Unfortunately, the global palaeomagnetic reconstructions cannot help in this debate as they cannot clearly reproduce such rapid variations, mainly due to the sparse and uneven global data distribution and the uncertainties in their dating (Korte and Constable, 2018). The contribution of new, high quality and well dated archaeomagnetic data from Eastern Mediterranean and Middle East is thus very important to explore the geographical and temporal distribution of such geomagnetic field anomalies. Even though great effort has been focused on the acquisition of new intensity records from these areas (e.g. Ben-Yosef et al., 2011; Shaar et al., 2015; Gallet et al., 2015), the directional data obtained from the study of *in situ* baked clay structures are still very few (e.g. Speranza et al., 2006; Tema et al., 2018; Ertepinar et al., 2019). For this purpose, we present here new directional archaeomagnetic data from Cyprus, in order to enrich the reference directional dataset in the Eastern Mediterranean and contribute to the investigation of the directional occurrence of the Middle East anomaly in areas near to Israel, such as Cyprus.

2. Archaeological context and sampling

Archaeomagnetic samples were collected from 13 *in situ* baked clay structures, coming from 5 different archaeological sites in Cyprus: Marki-Alonia, Idalion, Athienou-Malloura, Palaion Demarcheion (Lefkosia) and Agios Georgios (Lefkosia) (Fig. 1a).

2.1 Archaeological sites

- *Marki-Alonia (MKA).*

The Marki Alonia archaeological site (35.02^{o} N, 33.33^{o} E) is situated in central Cyprus, 15 km south of the capital Lefkosia, and was excavated by the Australian Cyprus Expedition during several seasons from 1990 to 2000. The excavations revealed an extended Bronze Age settlement, occupied for several centuries from the Bronze Age (about 2400 BCE) to the Middle Cypriot II (about 1800 BCE) (Frankel and Webb, 2000). Within the excavated area several architectural households have been identified. Most of them consist of yards with enclosed small rooms, where hearths and clay ovens were often found (Frankel and Webb, 2006). Clear evidence of rebuilding and frequent renovation of the structures suggests a complex history of the site. However, the relatively fine-scale changes recognized in the excavated area contributed to the division of the development of the Marki sequence into nine phases, based on stratigraphic, architectural and ceramic evidence (Frankel and Webb, 2006). For this study, we sampled the wall of a small oven originally built in Phase C (Context 1897), and then rebuilt and remodeled in Phase D (Context 3346) (Frankel and Webb 2006: 22, pl. 10e–f). The oven (Fig. 1b) was last used after its reconstruction and can thus be dated in the Early Cypriot Phase II, around 2150-2050 BCE.

- *Idalion (IDN).*

The ancient city of Idalion (35.02 ^{o}N, 33.42 ^{o}E) is situated in the Mesaoria Plain, near to the village of Dhali, about 25 km south-east of Lefkosia. The excavations conducted in the area

since the middle of the 19th century, revealed rich architectural, numismatic and epigraphic findings. The Idalion city-kingdom was founded by Eteocypriots around 1220 BCE but it reached its greatest prosperity during the 7th and 6th centuries. In 450 BCE the city was occupied by Phoenicians, who held it until the Hellenistic occupation around 300 BCE and it eventually declined under their rule. The archaeological excavations brought to light a large number of coins attributed to the Kings of Idalion, sculptures, inscriptions, as well as a large collection of pottery and remains of metallurgical activity (Hadjicosti, 1997). In this study, a large sunken dolia (Str. 3, Square 10) was sampled (Fig. 1c). According to the stratigraphic information and the diagnostic pottery found in the surrounding area, the structure was dated at 1200-1050 BCE.

- *Athienou-Malloura (MLR).*

The Athienou-Malloura archaeological site (35.08 ^{o}N, 33.58 ^{o}E) is situated around 6 km southwest of the village of Athienou, in Larnaca district, halfway between Lefkosia and Larnaca. Archaeological excavations have been conducted since 1990, coordinated by the American archaeological team of the University of Davidson (North Carolina, USA). The excavations brought to light important archaeological finds comprising two cemeteries (one from the Archaic to the Roman period and the other from the Venetian), a settlement (from the Roman to Ottoman Period) and a sanctuary of male gods (from the Archaic to the Roman period). The thousands of objects and artifacts found at the site reveal the rich archaeological heritage of the area. In the present study, a baked clay wall in sector 32 and a flat hearth in sector 14 were sampled (EU28-MLR1 and EU94-MLR2, respectively). The former was almost certainly part of a domestic oven while the latter was likely a hearth or an altar (Fig. 1d). According to archaeological evidence based on ceramics they are dated to the Cypro-Archaic II (600-480 BCE) and Cypro-Archaic I (750-600 BCE) periods, respectively.

- *Palaion Demarcheion, Lefkosia (PLND).*

149 The archaeological site of Palaion Demarcheion (35.17 ^{o}N, 33.37 ^{o}E) is situated in the
150 center of the old city of Lefkosia, within the Venetian walls. The emplacement was used as a
151 municipal car-park since the 1960's and the archaeology was discovered in 2002 when the area
152 was cleared for the construction of the new Lefkosia City Hall. Rescue excavations were
153 conducted by the Department of Antiquities from June 2002 up to October 2006. The excavated
154 areas revealed a part of the Byzantine and medieval city, including churches with cemeteries,
155 monumental buildings, many workshop areas (for the production of glass, jewelry and pottery) and
156 other architectural remains. The rich findings indicate that the site was occupied from the 11th to
157 the 20th centuries CE (Chrysostomou and Violaris, 2018). The architectural remains of two
158 churches, each associated with a cemetery, are perhaps amongst the most important findings of the
159 excavations. The foundations of the northern part of the first church (Church A) are associated
160 with pottery dating to the 12th century CE, while the southern part has two architectural phases that
161 date to the second half of the 12th century or the beginning of the 13th century CE. The second
162 church (Church B) is associated with an architectural phase that dates towards the end of the 11th
163 or early 12th century CE, and burials surrounding the church date at least from the 12th century
164 (Chrysostomou and Violaris, 2018). During the early 13th century, Church B was destroyed by fire,
165 it was rebuilt, but it was subsequently destroyed again. In this study a flat domestic hearth
166 (PLND1) excavated in square L6-D and a small circular metallurgical hearth (PLND2) excavated
167 in square M6 were sampled (Fig. 1e), dated at 13th-14th centuries CE and 12th century CE,
168 respectively, based on the stratigraphy and archaeological finds.

169 - *Agios Georgios, PA.SY.D.Y., Lefkosia (PSY).*

170 The archaeological site of Agios Georgios (known as PA.SY.D.Y) is situated on the hill of
171 Agios Georgios (35.17^{o} N, 33.35^{o} E), in central Lefkosia. Excavations began in 1996, following
172 the decision to build the new House of Representatives on the site. Excavations were then carried
173 out from 1996 to 2006, revealing an extensive settlement that included workshop areas for the

manufacture of terracotta, limestone and metal objects. Occupation of the site dates from the Archaic period to the end of the Hellenistic period. Furthermore, some remains assignable to the early Christian period until the 16th century CE were also found. In this study, our sampling was focused on the baked clay ovens and hearths found at the site, in the areas VI, XI, XII, XIII, XVI (Pilides et al., 2007). In particular, oriented samples were collected from seven baked clay structures: structure 13 (PSY1), 15a (PSY2), 60 (PSY3), 21 (PSY4), 65 (PSY5), 55 (PSY6) and 61a (PSY7). Most of the structures studied were circular ovens (Fig. 2) or metal-working installations (Pilides et al., 2007). Even though the exact time of the last firing of each one of the sampled hearths is difficult to ascertain and will be the aim of a future detailed archaeological study, they all belong to Late Classical and Hellenistic periods based on coin and ceramic finds. They can thus be safely dated from the end of the 4th century BCE to the half of the 1st century BCE.

2.2 *In-situ* magnetic susceptibility mapping of the Agios Georgios hearths

In the case of Agios Georgios, a Bartington MS2 portable magnetic susceptibility meter with an F-type probe was first used to measure the variation of the initial magnetic susceptibility on the surface of three of the flat hearths. A detailed magnetic image of each hearth can provide evidence as to its function in antiquity. The variation of the magnetic susceptibility can also be useful to define those parts that were better fired and thus more suitable for archaeomagnetic sampling, taking into consideration that firing leads to an enhancement of the magnetic susceptibility (Jordanova et al., 2001; Carrancho and Villalain, 2011; Tema and Ferrara, 2019).

The sensitivity of the F-probe deceases rapidly with distance such that 90% of the signal comes from a 6 mm depth below the flat tip of the sensor (manufacturer's specification). As measurements on experimental fires have shown that the maximum temperature achieved decreases rapidly with depth (Linford et al., 2001), the F-probe was ideally suited to examine the magnetic susceptibility variation on the Agios Georgios flat hearths.

Magnetic susceptibility mapping revealed an inhomogeneous pattern indicating that some parts of the studied hearths had been heated at higher temperatures (Fig. 2). Our survey shows that the maximum susceptibility values are not concentrated in the center of the hearths, as would be expected and observed in previous studies (Morinaga et al., 1999). The PSY1 hearth shows a pronounced maximum susceptibility at the south-west side, where the baked clay was also characterized by a darker color (Fig. 2 a, b). Similarly, the PSY2 hearth shows an asymmetrical magnetic susceptibility variation with higher values at the northern part, although without any clear difference in color of the baked clay. (Fig. 2 c, d). PSY4 hearth is the least magnetic of the hearths studied, with maxima at the south and north edges (Fig. 2 e, f).

Distinct areas of higher magnetic susceptibility (hot spots) on the surface of these hearths would suggest the use of a controlled air draft or even some form of forced ventilation (Rehder, 1994). This is compatible with the evidence of metal working at the Agios Georgios site. The susceptibility values registered in all surveyed structures are high, suggesting the suitability of the structures for archaeomagnetic investigation.

2.3 Archaeomagnetic sampling

Archaeomagnetic sampling was carried out during several field campaigns made between 1999 and 2006. In all cases, following the magnetic susceptibility survey results, samples were collected from the parts of the structures that showed evident signs of heating. Generally, the upper parts of the structures' floors or the lower parts of the walls seemed to be better baked and were thus preferred. Oriented samples suitable for a directional investigation were collected by gluing 22 mm diameter plastic disks on the baked clay's upper surface. The orientation of the horizontal line drawn on each disc was measured using a Brunton compass and an Anglestar electronic clinometer. A sun compass was also used, in order to correct the azimuth of the samples for any local magnetic disturbance. Between 7 and 19 independently oriented samples were collected from each structure.

3. Methods

The bulk magnetic susceptibility and the Natural Remanent Magnetization (NRM) of most of the samples were measured shortly after sampling at the Petrophysics Laboratory, Geneva University (Switzerland) with a Bartington MS2B susceptibility meter and a Minispin magnetometer. The structures MLR2, PSY3 and PSY5 showed very low Q-ratio values, Qn, ($0.6 < Qn < 1.8$) as well as very dispersed NRM directions, suggesting insufficient heating to acquire a stable and representative ancient geomagnetic field record; they were therefore excluded from any further analysis. For all the remaining structures, samples were systematically stepwise demagnetized at the Alpine Palaeomagnetic Laboratory (ALP), at Peveragno (Italy) with a D-2000 ASC demagnetizer and their magnetic remanence was measured with a JR6 Spinner magnetometer (AGICO). The magnetic anisotropy of representative samples was investigated with a KLY3 Kappabridge (AGICO). Magnetic mineralogy experiments including Isothermal Remanent Magnetization (IRM) acquisition and back field curves, magnetic moment monitoring up to 700 ^{o}C, and hysteresis loops were carried out at the ALP laboratory and at the Istituto Nazionale di Ricerca Metrologica (INRIM), at Torino (Italy). Hysteresis loops and thermomagnetic curves were measured at INRIM with a Lake Shore 7400 Vibrating Sample Magnetometer (VSM) equipped with a thermo-resistance oven operating in an inert Argon atmosphere on small fragments (mass < 100 mg).

4. Results

4.1 Magnetic mineralogy

The IRM curves obtained for one sample from each structure show that saturation is reached in all cases at applied fields of around 0.2-0.4 T (Fig. 3a), suggesting the presence of a

low-coercivity mineral. The back-field curves also indicate the presence of a soft magnetic mineral with remanence coercivity being in all cases lower than 50 mT, except for sample PSY7-2 coming from the more vitrified structure 61, that is characterized by a higher coercivity (Fig. 3b). Hysteresis loops (corrected for the para/diamagnetic contributions) further confirm these results (Fig. 3c). They indicate the presence of soft magnetic minerals, such as magnetite and Ti-magnetite, as the main carriers of the magnetic moment. This is assumed from the tight shape of the hysteresis loops accompanied by low coercive fields: H_c values are in the range 5- 15 mT except from sample PSY 7-2 that has higher H_c of around 35 mT, as already indicated by the IRM back field curve. The magnetic parameters provided by the hysteresis loops of representative samples (i.e. coercive field H_C, magnetic remanence M_{RS}, and magnetic saturation M_S) together with the remanence coercivity values, H_{CR}, provided by the back-field curves, were plotted on a Day Plot (Fig. 3d). All samples show magnetic granulometry that fits in the pseudo single domain (PSD) part of the Day plot (Dunlop, 2002). Thermomagnetic curves of the magnetic moment versus temperature up to 600 ◦C or 700 ◦C show Curie temperatures of around 580 ^{o}C, indicating the presence of magnetite as the main magnetic mineral (Fig. 4). In most cases they are not reversible, with cooling curves being always higher, probably due to the formation of new minerals during heating. Such curves also suggest that the heating temperatures experienced by the baked structures during their use were probably lower than 600-700 °C.

4.2. Magnetic anisotropy

Archaeological structures and artifacts such as kilns, tiles, bricks and pottery can in some cases be highly anisotropic and several studies have shown that their pronounced magnetic fabric may influence not only their archaeointensity values but also the direction of the recorded geomagnetic field vector (Hus et al., 2003; Tema, 2009; Palencia-Ortas et al., 2017). Generally, baked clays from small hearths, ovens and fireplaces are not anisotropic (e.g. Kovacheva et al., 2009; Tema et al., 2016). However, to investigate any possible deviation of the ChRM direction in

the samples studied here, we have measured the anisotropy of the magnetic susceptibility (AMS) on 44 samples from Idalion (IDN), Athienou-Malloura (MLR1 and MLR2) and Marki-Alonia (MKA). The mean anisotropy parameters (L: magnetic lineation; F: magnetic foliation; P: degree of anisotropy; T: shape factor) are obtained according to Jelinek (1981) using the Anisoft software (Table S.1, Supplementary material). The AMS degree (P_{AMS}) is in all cases very low, varying from P_{AMS}= 1.001 for Idalion to P_{AMS}=1.018 for Marki. These results confirm that the anisotropy of baked clays coming from unmodeled structures like small hearths is very low and it should not influence the magnetic direction recorded by the clays during their last firing.

4.3 Archaeomagnetic direction

The results of the stepwise AF demagnetization experiments were plotted in equal area projections, intensity decay curves and Zijderveld diagrams (Zijderveld, 1967) and were interpreted using the Remasoft3.0 software. The results obtained generally show linear Zijderveld diagrams and the Characteristic Remanent Magnetization (ChRM) component is easily and clearly isolated (Fig. 5). Secondary components, if any, are cancelled during the first steps of the AF demagnetization, usually at fields <20 mT. The direction of the ChRM at sample level was calculated according to principal component analysis while the mean direction for each structure studied was obtained assuming a Fisherian distribution (Fisher, 1953). In all cases the mean directions are very well defined (Fig. 6) and characterized by small α_{95} angles of confidence ($\alpha_{95} \leq$ 3.1 ^{o}) and high precision parameter, k, (k> 150), apart from the structures PLND1, PSY-4 and PSY-7 that are characterized by more dispersed directions and thus higher α_{95} values. The obtained directions at structure level are given in Table 1, together with their archaeological age.

5. Discussion

5.1 New directional data from Cyprus

297 The first archaeomagnetic directional data from Cyprus came from seven *in situ* baked clay
298 structures excavated at the copper smelting site of Agia Varvara-Almyras (Tema et al., 2018). No
299 other directional data are available so far, even though Cypriot slags and ceramics have been
300 successfully used for archaeointensity studies (e.g. Shaar et al., 2015; Ertepinar et al., 2020). The
301 new directions presented in this study aim to enrich this scant directional dataset whilst the data
302 from the Palaion Demarcheion archaeological site are actually the only directional records from
303 Cyprus for the last 2000 years.

304 Due to the very limited directional data from Cyprus, we compare our new data with
305 published data from sites in the Middle East and Anatolia, both areas known to be characterized by
306 extreme geomagnetic field variability (e.g. Shaar et al., 2018; Ertepinar et al., 2020). Shaar et al.
307 (2018) recently published an extensive catalogue of archaeomagnetic directional records from
308 Israel. This catalogue includes 76 directions; 47 of them are classified as of high quality, satisfying
309 selection criteria based on the number of specimens and statistical quality parameters (Shaar et al.,
310 2018). The most prominent feature of these data is the high declination and inclination values
311 observed at the beginning of the first millennium BCE while they also show other periods with fast
312 secular variation rates. Apart from Israel, more directional data are available from countries
313 neighboring Cyprus such as Turkey (Ertepinar et al., 2012; 2016; 2020) and Syria (Speranza et al.,
314 2006). More recently, Ertepinar et al. (2020), published new archaeomagnetic data from the
315 Eastern Mediterranean, including directional results from four archaeological sites in Turkey with
316 ages ranging from 3300 BCE to 672 BCE, and with intensity data from both Turkey and Cyprus
317 that further support extreme field variations in the region.

318 In order to compare our data with the directional data from the literature, we have relocated
319 them to the geographical coordinates of Lefkosia (35.17 °N, 33.36 °E) using the virtual
320 geomagnetic pole method (Noel and Batt, 1990). The new data from Agios Georgios
321 archaeological site are in good agreement with literature data from Agia Varvara (Tema et al.,

2018) and Israel (Shaar et al., 2018), apart from the PSY4 hearth that shows much lower inclination than the other contemporaneous records (Fig. 7). The data from Idalion and from Athienou-Malloura are also in agreement with data from Israel and they seem to support the presence of a short lived Levantine anomaly, showing increasing declination and inclination values before the peak values observed at Israel around 1000-900 BCE, and a clear decreasing trend after that period. Data from Marki, dated around 2000 BCE, show a low declination with respect to slightly younger data from Turkey, even though the inclination fits well with the Turkish data. Unfortunately, there are no available data for the 10-14th centuries CE to compare the new records from Palaion Demarcheion. However, they seem to show a high declination around 1100 CE and a low inclination around 1300 CE, following a general trend suggested by the Israeli data (Fig. 7).

5.2 Directional Secular Variation path in Eastern Mediterranean and Middle East

The geographical position of Cyprus, situated between Turkey, Syria and Israel, makes it particularly interesting for reconstructing the Secular Variation path in the area of Eastern Mediterranean and Middle East. This area is of great geomagnetic interest due to the Levantine anomaly characterized by unusual high intensities. To investigate the directional occurrence of such anomaly and to explore other eventual abrupt directional changes in this area, we have calculated a directional SV curve based on the new and previously published archaeomagnetic reference data from Cyprus, Israel, Turkey and Syria. To guarantee internal consistency to the reference dataset, we adopted the selection criteria applied by Shaar et al. (2018) to the Israel data and we therefore rejected all data that are based on less than 8 specimens, have age error more than 100 years and α_{95} angle of confidence greater than 6^{o}. As well as the archaeomagnetic data, historical directional data from the HISTMAG database (Arneitz et al., 2017), located within a circular area of 600 km radius around Lefkosia, were also used to better constrain the geomagnetic field path during the last few centuries. All data are relocated to Lefkosia (35.17 °N, 33.36 °E) via the pole method.

347 The new time-continuous directional SV curve was computed following the method
348 described by Molina-Cardin et al. (2018), where a local paleomagnetic full-vector $\vec{M}$ is modeled
349 by means of penalized cubic b-splines in time. Since the available data cover the last 4 millennia,
350 we fixed the temporal basis of splines every 25 years within a time window from 2000 BCE to
351 1900 CE. It is worth noting that the paleomagnetic full-vector includes all the palaeofield
352 elements, i.e., declination, inclination and intensity, while our study is only focused on directional
353 data. To solve the lack of the intensity, we normalized the vector of the unknown coefficients $\vec{C}$ by
354 the first coefficient c_1 (see Text S3 of the Supplementary material in Molina-Cardin et al., 2018),
355 providing a complete solution for both declination and inclination. The final time-continuous curve
356 is obtained by choosing an optimal damping parameter in the modeling inversion providing the
357 best fitting in terms of curve complexity and data residual. In addition, the curve uncertainties
358 were estimated by applying a bootstrap approach, using both random homogeneous and Gaussian
359 distributions based on the dating and measurement errors, respectively (for historical data a
360 constant α_{95} of 0.25º was assumed without a dating error). The directional curve computed is given
361 in Table S.2 (Supplementary material).

362 The new curves for declination and inclination are plotted in Figure 8 along with the
363 reference historical measurements and the selected reference archaeomagnetic data. They are the
364 first directional curves available for Cyprus and they are valid for the investigation of the
365 geomagnetic field's behavior in the area of Eastern Mediterranean and Middle East. For the last
366 two millennia, the new curves show high declination values around 200 CE, 600 CE and 1200 CE
367 and clearly low inclination values around 200 CE and 1300 CE. However, for the last 2000 years
368 the available high-quality data are quite scarce, and the low and high peaks seen in the curves are
369 constrained by only few data. On the contrary, the curves during the first two millennia BCE are
370 well detailed, and they clearly show high inclination values around 900 BCE, accompanied by
371 eastern declinations of around 10^{o}. Although single declination values are as high as 25^{o} the curves

372 do not show a clear declination peak due to the dispersion of the declination data for this period. It
373 is also interesting to note a clear low inclination observed around 1800 BCE, accompanied by
374 slightly western declination of around -5^{o}.

375 To further explore these aspects, we have compared our curves with the predictions of
376 some of the most recent global paleomagnetic field models (Fig. 8). Such paleomagnetic
377 reconstructions use all the available palaeomagnetic data spanning the last few millennia to
378 provide a time-continuous picture of the past geomagnetic field at any location over the Earth's
379 surface. Some of them are based on a combination of archaeomagnetic, volcanic and sediment
380 data, such as the pfm9k.1b (Nilsson et al., 2014) and the HFM.OL1.AL1 (Constable et al., 2016)
381 models, while others have excluded sediment data due to their known smoothed and post
382 depositional time-delay problems, using only archaeomagnetic and volcanic data (e.g.
383 SHA.DIF.14k, Pavón-Carrasco et al., 2014; ARCH10k.1, Constable et al., 2016; and the SHAWQ-
384 family, Campuzano et al., 2018 and Osete et al., 2019). All the cited global models cover the last
385 four millennia, except from the SHAWQ-family that only spans the last three millennia.
386 Comparison of our new curves with these models shows that during the last two millennia the
387 inclination curve is in good agreement with the models' predictions while the declination peaks of
388 around 200 CE and 600 CE are not seen in any of the models. For the BCE period, our new curves
389 show a better agreement with the SHAWQ-family model, even if the agreement with the
390 SHA.DIF.14k and ARCH10K.1 models can also be considered to be satisfactory.

391 5.3 Directional occurrence of LIAA and abrupt directional changes

392 With a view to further analyze the directional changes of the palaeofield in Cyprus and also
393 to investigate the directional occurrence of the LIAA, we have plotted the new curves in Bauer
394 plots of declination and inclination for 4 different time periods (Fig. 9a). Furthermore, we have
395 also calculated the curvature of the curve (Fig. 9b), to detect periods with rapid directional
396 changes. From 2000 BCE to 1000 BCE, the SV curve shows an east-west zigzag pattern in

declination with a continuous increase of inclination. In this millennium, the most abrupt change occurs around 1400 BCE (Fig. 9), when the curvature parameter reaches its maximum value. For the first millennium BC (1000 BCE – 0 CE) the declination swings to the west with abrupt changes around 900 BCE, 600 BCE and 200 BCE (Fig. 9a, b). The first event at 900 BCE is characterized by the highest curvature parameter and the highest inclination values of the last 4 millennia. The first millennium CE (0 CE – 1000 CE) is also characterized by west-east zigzag declination values with increasing inclinations, with some peaks in the curvature parameter around 0 CE, 250 CE and 800 CE. Finally, the last millennium (1000 CE – 1900 CE) shows a westward drift in the declination values with inclinations ranging between 50º and 60º without important abrupt changes, as shown by the close-to-zero curvature parameter (Fig. 9).

The Bauer plots and the curvature calculation presented here successfully show several abrupt directional variations with the most prominent characteristic of the directional SV in Cyprus during the last four millennia being the maximum curvature change depicted around 900 BCE. Such important curvature change can be clearly associated with the LIAA, confirming that apart the extreme intensity values, the geomagnetic field at that time was simultaneously characterized by very steep inclinations and directional variation. To quantify the directional variation around 900 BCE, we used the new curves to estimate the temporal rates before and after the curvature maximum. Before 900 BCE the declination is characterized by a rate of +3.2º/century moving towards east, and an increase rate of +1.8º/century for the inclination. After the maximum curvature, the declination moves towards the west with a rate of -5.7º/century while the inclination decreases around -3.6º/century. If we calculate such rates using the reference data themselves, instead of the curves, the temporal rates obtained are even higher as the curves are inevitably affected by some smoothing. Indeed, in this case before 900 BCE the declination changes by +7.0º/century and the inclination increases by +5º/century, while after 900 BCE the declination moves from east to west at a rate of 13.2º/century and the inclination decreases by -7.4º/century.

Such temporal change ranges are quite high and similar to those reported in Iberian Peninsula (Osete et al., 2020).

Apart from the 900 BCE directional change, the curvature peak observed around 600 BCE could be related to the high intensity values observed in Western Europe (Osete et. al, 2020) while the curvature change at 200 CE seems to perfectly coincide with the one observed by Gallet et al. (2003). Even though detecting rapid directional fluctuations from regional SV curves is often hard, due to the reference data uncertainties and to the smoothing introduced during computational processes (Le Goff and Gallet, 2019), it would be interesting to further investigate these important directional changes with new data, and if possible with full-geomagnetic field records (including both directional and intensity determinations).

6. Conclusions

We present 10 new directional data from Cyprus from 5 archaeological sites with ages ranging from 2000 BCE to 1400 CE. These new directions enrich the reference data for Cyprus and together with data from nearby Israel, Turkey and Syria are used to reconstruct the directional geomagnetic field path in the area of Eastern Mediterranean and Middle East during the last four millennia. A time-continuous SV curve was computed and used to investigate the directional occurrence of the LIAA anomaly and abrupt directional changes. Our investigation shows a maximum curvature change peak at around 900 BCE, confirming the hypothesis that the LIAA was accompanied by an abrupt directional change. Other important directional changes are also observed in several other BCE periods while during the last two millennia CE, the most important change is observed around 200 CE. Further investigation of these changes in curvature is still needed to better understand their non-dipole origin and explore their connection with intensity maxima.

Acknowledgments

I.H. kindly acknowledges Walter Fasnacht for his help during the 2006 sampling campaign at Agios Georgios. Maria Hadjicosti is also sincerely acknowledged for her contribution during sampling at Idalion.

References

Arneitz, P., Leonhardt, R., Schnepp, E., Heilig, B., Mayrhofer, F., Kovacs, P., Hejda P., Valach, F., Vadasz, Hammerl, C., Egli, R., Fabian, K., Kompein, N., 2017. The HISTMAG database: combining historical, archaeomagnetic and volcanic data. Geophysical Journal International, 210 (3), 1347-1359.

Ben-Yosef, E., Tauxe, L., Levy, T.E., Shaar, R., Ron, H., Najjar, M., 2009. Geomagnetic intensity spike recorded in high resolution slag deposit in southern Jordan. Earth Planet. Sci. Lett., 287, 529-539.

Ben-Yosef, E., Shaar, R., Tauxe, L., Levy, Th., Kassianidou, V., 2011. The Cyprus Archaeomagnetic Project (CAMP): targeting the slag deposits of Cyprus and the Eastern Mediterranean. Antiquity, 85, 1-5.

Campuzano, S.A., Gómez-Paccard, M., Pavón-Carrasco, F.J., Osete, M.L., 2019. Emergence and evolution of the South Atlantic Anomaly revealed by the new paleomagnetic reconstruction SHAWQ2k. Earth and Planetary Science Letters, 512, 17-26.

Carrancho, A., Villalain, J.J., 2011. Different mechanisms of magnetisation recorded in experimental fires: Archaeomagnetic implications. Earth and Planetary Science Letters, 312, 176-187.

Chrysostomou, P., Violaris, Y., 2018. Palaeodemographic Analysis of a Byzantine-Medieval Neighbourhood in Nicosia, Palaion Demarcheion ('Old Municipality') 2002-2004. Archeologia Cypria, VII, 135-161, ISSN 0257-1951

Constable, C., Korte, M., Panovska, S., 2016. Persistent high paleosecular variation activity in southern hemisphere for at least 10 000 years. Earth and Planetary Science Letters, 453, 78-86.

Davies, C., Constable, C., 2017. Geomagnetic spikes on the core-mantle boundary. Nature communications, 8, 15593. https://doi.org/10.1038/ncomms15593.

Dunlop, D. J. 2002, Theory and application of the Day plot (Mrs/Ms versus Hcr/Hc) 1. Theoretical curves and tests using titanomagnetite data. J. Geophys. Res., 107 (B3), 2056.

Ertepinar, P., Langereis, C.G., Biggin, A.J., Frangipane, M., Matney, T., Ökse, T., Engin, A., 2012. Archaeomagnetic study of five mounds from upper Mesopotamia be-tween 2500 and 700BC: further evidence for an extremely strong geomagnetic field ca. 3000 years ago. Earth Planet. Sci. Lett., 357, 84-98.

Ertepinar, P., Langereis, C.G., Biggin, A.J., de Groot, L.V., Kulakoˇglu, F., Omura, S., Süel, A., 2016. Full vector archaeomagnetic records from Anatolia between 2400 and 1350 BCE: implications for geomagnetic field models and the dating of fires in antiquity. Earth Planet. Sci. Lett., 434, 171-186.

Ertepinar, P., Hammond, M.L., Hill, M.J., Biggin, A.J., Langereis, C.G., Herries, A.I.R., Yener, K.A., Akar, M., Gates, M. H., Harrison, T., Greaves, A.M., Frankel, D., Webb, J.M., Özgen, I., Yazicioglu, G.B., 2020. Extreme geomagnetic field variability indicated by Eastern

504 Mediterranean full-vector archaeomagnetic records. Earth Planet. Sci. Lett., 531,
505 https://doi.org/10.1016/j.epsl.2019.115979
506
507 Fisher R.A., 1953. Dispersion on a sphere. Proc. R. Soc. London A, 217, 295-305.
508
509 Frankel, D., Webb, J.M., 2000. Marki Alonia: a prehistoric Bronze Age settlement in Cyprus.
510 Antiquity, 74, 763-64.
511
512 Frankel, D., Webb, J.M., 2006. Neighbors: Negotiating space in a prehistoric village. Antiquity,
513 80, 287-302.
514
515 Gallet, Y., Genevey, A., Courtillot, V., 2003. On the possible occurrence of 'archaeomagnetic
516 jerks' in the geomagnetic field over the past three millennia. Earth Planet. Sci. Lett., 214, 237-
517 242.
518
519 Gallet, Y., Molist, M., Genevey, A., Clop Garcia, X., Thébault, E. Gómez, Bach, A., Le Goff, M.,
520 Robert, B., Nachasova, I., 2015. New Late Neolithic (c. 7000–5000 BC) archaeointensity data
521 from Syria. Reconstructing 9000 years of archaeomagnetic field intensity variations in the Middle
522 East. Phys. Earth Planet. Inter., 238, 89-103.
523
524 Gómez-Paccard, M., Osete, M. L., Chauvin, A., Pavón-Carrasco, F. J., Pérez-Asensio, M.,
525 Jiménez, P., Lanos, Ph., 2016. New constraints on the most significant paleointensity change in
526 Western Europe over the last two millennia. A non-dipolar origin? Earth and Planetary Science
527 Letters, 454, 55-64.
528

Hervé, G., Fabbinder, J., Gilder, S., Metzner-Nebelsick, C., Gallet, Y., Genevey, A., 2017. Fast geomagnetic field intensity variations between 1400 and 400 BCE: New archeointensity data from Germany. Physics of the Earth and Planetary Interiors, 270, 143-156.

Jackson, A., Finlay, C., 2015. Geomagnetic secular variation and its applications to the core. Treatise on Geophysics (Second Edition), 5, 137-181. https://doi.org/10.1016/B978-0-444-53802-4.00099-3

Jelinek, V., 1981. Characterization of the magnetic fabric of rocks. Tectonophysics, 79, 63–67.

Jordanova, N., Petrovsky, E., Kovacheva, M., Jordanova, D., 2001. Factors determining Magnetic Enhancement of Burnt Clay from Archaeological Sites. Journal of Archaeological Science, 28, 1137-1148.

Hadjicosti, M., 1997. The Kingdom of Idalion in the light of the New Evidence. In: The City-Kingdoms of Early Iron Age Cyprus in their Eastern Mediterranean Context, Bulletin of the American Schools of Oriental Research, 308, 49-63.

Hus, J., Ech-Chakrouni, S., Jordanova, D., Geeraerts, R., 2003. Archaeomagnetic investigation of two mediaeval brick constructions in North Belgium and the magnetic anisotropy of bricks. Geoarchaeology, 18, 225-253.

Korte, M., Constable, C., 2018. Archaeomagnetic intensity spikes: Global or regional geomagnetic field features? Frontiers in Earth Science, 6, 17. https://doi.org/10.3389/feart.2018.00017

555 Kovacheva, M., Chauvin, A., Jordanova, N., Lanos, Ph., Karloukovski, V., 2009. Remanence
556 anisotropy effect on the palaeointensity results obtained from various archaeological materials,
557 excluding pottery. Earth Planets Space, 61, 711-732.
558
559 Le Goff, M., Gallet, Y., 2019. On the resolution of regional archaeomagnetism: Untangling
560 directional geomagnetic oscillations and data uncertainties using the French archaeomagnetic
561 database for between 1000 and 1500 AD as a guide. Geological Society of London. Journal
562 contribution. https://doi.org/10.6084/m9.figshare.10265306.v1
563
564 Linford, N.L., Canti, M.G., 2001. Geophysical evidence for fires. Archaeol. Prospect., 8, 211-
565 225.
566
567 Livermore, P. W., Fournier, A., Gallet, Y., 2014. Core-flow constraints on extreme
568 archaeomagnetic intensity changes. Earth Planet. Sci. Lett., 387, 145-156.
569
570 Molina-Cardín, A., Campuzano, S.A, Osete, M.L., Rivero-Monter, M., Pavón-Carrasco, F.J.,
571 Palencia-Ortas, A., Martín-Hernández, F., Gómez-Paccard, M., Chauvin, A., Guerrero-Suárez, S.,
572 Pérez-Fuentes, J.C., McIntosh, G., Catanzariti, G., Sastre Blanco, J.C., Larrazabal, J., Fernández
573 Martínez, V.M., Álvarez Sanchís, J.R., Rodríguez-Hernández, J., Martín Viso, I., Garcia i Rubert,
574 D., 2018. Updated Iberian Archeomagnetic Catalogue: New Full Vector Paleosecular Variation
575 Curve for the Last 3 Millennia. Geochemistry, Geophysics, Geosystems, 19 (10), 3637-3656.
576
577 Morinaga, H., Inokuchi, H., Yamashita, H., Ono, A., Takashi, I., 1999. Magnetic detection of
578 heated soils at Paleolithic sites in Japan. Geoarchaeology, 14 (5), 377-399.
579

Nilsson, A., Holme, R., Korte, M., Suttie, N., Hill, M., 2014. Reconstructing Holocene geomagnetic field variation: new methods, models and implications. Geophys. J. Int., 198 (1), 229-248.

Noel, M., Batt, C.M., 1990. A method for correcting geographically separated remanence directions for the purpose of archaeomagnetic dating. Geophys. J. Int., 102, 753-756.

Osete, M.L., Molina-Cardín, A., Campuzano, S.A., Aguilella-Arzo, G., Barrachina-Ibáñez, A., Falomir-Granell, F., Oliver Foix, A., Gómez-Paccard, M., Martín-Hernández, F., Palencia-Ortas, A., Pavón-Carrasco, F.J., Rivero-Montero, M., 2020. Two archaeomagnetic intensity maxima and rapid directional variation rates during the Early Iron Age observed at Iberian coordinates. Implications on the evolution of the Levantine Iron Age Anomaly. Earth and Planetary Science Letters, 533, 116047.

Palencia-Ortas, A., Osete, M.L., Campuzano, S.A., McIntosh, G., Larrazabal, J., Sastre, J., Rodriguez-Aranda, J. 2017. New archaeomagnetic directions from Portugal and evolution of the geomagnetic field in Iberia from Late Bronze Age to Roman Times. Physics of the Earth and Planetary Interiors, 270, 183-194.

Pavón-Carrasco, F.J., Osete, M.L., Torta, J.M., De Santis, A., 2014. A geomagnetic field model for the Holocene based on archaeomagnetic and lava flow data. Earth Planetary Science Letters, 388, 98 - 109.

Pilides, D., Fasnacht, W., Peege, C., Hedley, I., Northover, P., Senn, M., 2007. A metallurgical installation on the Hill of Agios Georgios (PA.SY.D.Y.), Lefkosia. Report of the Department of Antiquities, Cyprus, 258-292.

606

607 Rehder J. E., 1994. Blowpipes versus bellows in Ancient Archaeology. Journal of Field
608 Archaeology, 21, 345-350.

609

610 Shaar, R., Ben-Yosef, E., Ron, H., Tauxe, L., Agnon, A., Kessel, R., 2011. Geomagnetic field
611 intensity: how high can it get? How fast can it change? Constraints from iron-age copper-slag.
612 Earth Planet. Sci. Lett., 301, 297-306.

613

614 Shaar, R., Tauxe, L., Ben-Yosef, E., Kassianidou, V., Lorentzen, B., Feinberg, J.M., Levy, T.E.,
615 2015. Decadal-scale variations in geomagnetic field intensity from ancient Cypriot slag mounds.
616 Geochemistry, Geophysics, Geosystems, 15 (1), 195-24.

617

618 Shaar, R., Tauxe, L., Ron, H., Ebert, Y., Zuckerman, S., Finkelstein, I., Agnon, A., 2016. Large
619 geomagnetic field anomalies revealed in Bronze to Iron Age archeomagnetic data from Tel
620 Megiddo and Tel Hazor, Israel. Earth Planet. Sci. Lett., 442, 173-185.

621

622 Shaar, R., Hassul, E., Raphael, K., Ebert, Y., Segal, Y., Eden, I., Vaknin, Y., Marco, S.,
623 Nowaczyk, N., Chauvin, A., Agnon, A., 2018. The first catalog of archaeomagnetic directions
624 from Isrlael with 4000 years of geomagnetic Secular Variations. Frontiers in Earth Sciences,
625 6:164, doi: 10.3389/feart.2018.00164.

626

627 Speranza, F., Maritan, L., Mazzoli, C., Morandi Nonacossi, D., D'Ajello Caracciolo, F., 2006.
628 First directional archaeomagnetic results from Syria: evidence from Tell Mishrifeh/Qatna.
629 Geophys. J. Int., 165, 47-52.

630

631 Tema, E., 2009. Estimate of the magnetic anisotropy effect on the archaeomagnetic inclination of
632 ancient bricks. Physics of the Earth and Planetary Interiors, 176, 213-223.
633
634 Tema, E., Ferrara, E., Camps, P., Conati Barbaro, C., Spatafora, S., Carvallo, C., Poidras, Th.,
635 2016. The Earth's magnetic field in Italy during the Neolithic period: new data from the Early
636 Neolithic site of Portonovo (Marche, Italy). Earth Planet. Sci. Lett., 448, 49-61.
637
638 Tema, E., Hedley, I., Fasnacht, W., Peege, C., 2018. Insights on the geomagnetic secular
639 variation in the Eastern Mediterranean: First directional data from Cyprus. Physics Earth and
640 Planetary Interiors, 285, 1-11.
641
642 Tema, E., Ferrara, E., 2019. Magnetic measurements as indicator of the equivalent firing
643 temperature of ancient baked clays: New results, limits and cautions. Journal of Cultural
644 Heritage, 35, 64-75.
645
646 Zijderveld J., 1967. AC demagnetization of rocks: analysis of results. In: Collinson D., Creer K.
647 and Runcorn S. (Eds), Methods in Palaeomagnetism. Elsevier, New York, 254-286.
648

649 **Figure captions**

650 Fig. 1 a) Location of the newly studied archaeological sites and photos of the structures from b)
651 Marki; c) Idalion; d) Malloura (MRK2); e) Palaion Demarcheion (PLND2).

652 Fig. 2 Photos of the studied structures (left) from Agios Georgios and maps of the in-situ measured
653 bulk magnetic susceptibility variations (right) from a, b) PSY1; c, d) PSY2 and e, f) PSY4.

654 Fig. 3 a) Representative Isothermal Remanent Magnetization (IRM) acquisition curves; b) back-
655 field IRM curves; c) hysteresis loops after correction for the para/diamagnetic contribution; d)
656 hysteresis ratios displayed on a Day plot (Dunlop, 2002).

657 Fig. 4 Magnetic moment vs temperature curves obtained for samples from a) PLND1; b) PLND2; c)
658 PSY1; d) PSY2; e) PSY6; f) MKA

659 Fig. 5 Stepwise alternative field demagnetization results plotted in orthogonal vector projections
660 (Zijderveld diagrams).

661 Fig. 6 Mean archaeomagnetic directions (red star) calculated for each structure, plotted in equal area
662 projections together with the alpha-95 angle of confidence (pink ellipsoid).

663 Fig. 7 Comparison of the new directional results for Cyprus with literature data from nearby
664 countries available for the last four millennia. All data are relocated at the geographic coordinates of
665 Lefkosia (35.17 °N, 33.36 °E).

666 Fig. 8 New paleosecular variation curves for a) declination and b) inclination for the Eastern
667 Mediterranean (dark red curves with error bands at 1 sigma of probability). Black and grey dots
668 represent the archaeomagnetic and historical data, respectively. Different color curves show the
669 global model predictions (see legend).

670 Fig. 9 a) Bauer diagram of the new paleosecular variation curve divided in four periods between
671 2000 BCE and 1900 CE. Declinations correspond to the meridian lines (from 30º W to 30º E

672 equally spaced every 5º), while inclinations are represented by the parallel curves (from 40º to 70º
673 equally spaced every 5º). Tie points every 200 years are indicated in the different panels, with
674 alternating red and yellow colors every century. b) Curvature of the paleosecular variation curve
675 assuming the projection of the directional paleomagnetic elements in a horizontal plane at the
676 Earth's surface.

677

678 **Table caption**

679 Table 1. Summary of the archaeomagnetic directions obtained from the studied structures.

680 Columns: Archaeological site; structure studied; Lat. (^{o}); Long. (^{o}); N= number of independently
681 oriented samples considered for the calculation of the mean direction; D= mean declination (◦); I=
682 mean inclination (◦); α_{95}= 95% semi-angle of confidence; k= precision parameter (Fisher, 1953);
683 archaeological age.

684

685 **Supplementary material**

686 Table S.1. Summary of the anisotropy of the magnetic susceptibility results.

687 Columns: Archaeological site; N= number of samples studied; L= magnetic lineation; F= magnetic
688 foliation; P= degree of anisotropy; T= shape parameter.

689

690 Table S.2. Palaeosecular Variation Curve for for Eastern Mediterranean and Middle East for the last
691 4 millennia.

692 Columns: Date (from 2000 BC to 1900 AD with step of 50 yr.); Declination value (º) and its
693 uncertainty (º) at 1-sigma of probability; Inclination value (º) and its uncertainty (º) at 1-sigma of
694 probability.

695

696

697

698

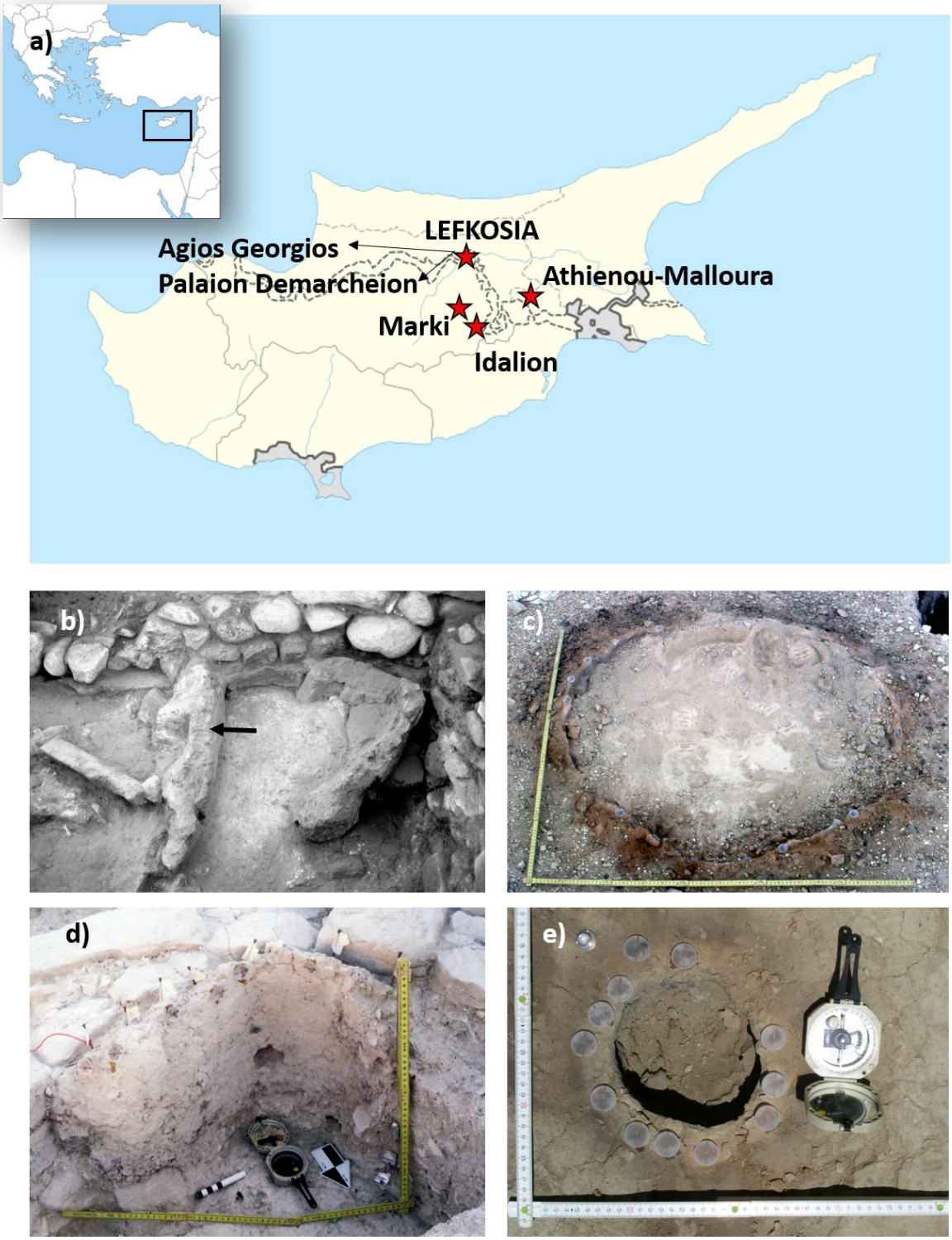
a)
LEFKOSIA
Agios Georgios
Palaion Demarcheion
Athienou-Malloura
Marki
Idalion
b)
c)
d)
e)

Fig. 1

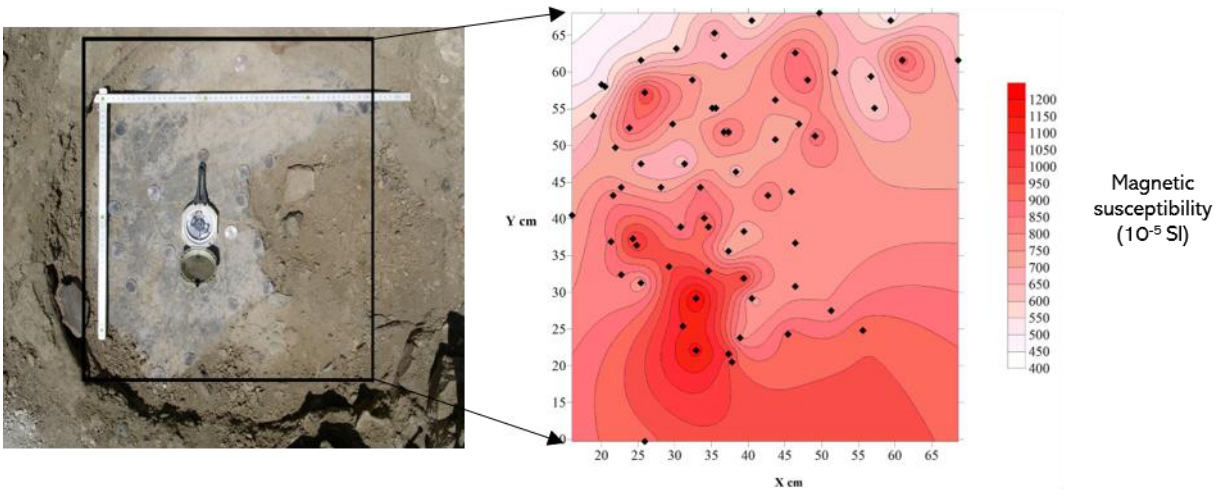
Y cm
X cm
Magnetic susceptibility (10-5 SI)

a) b)

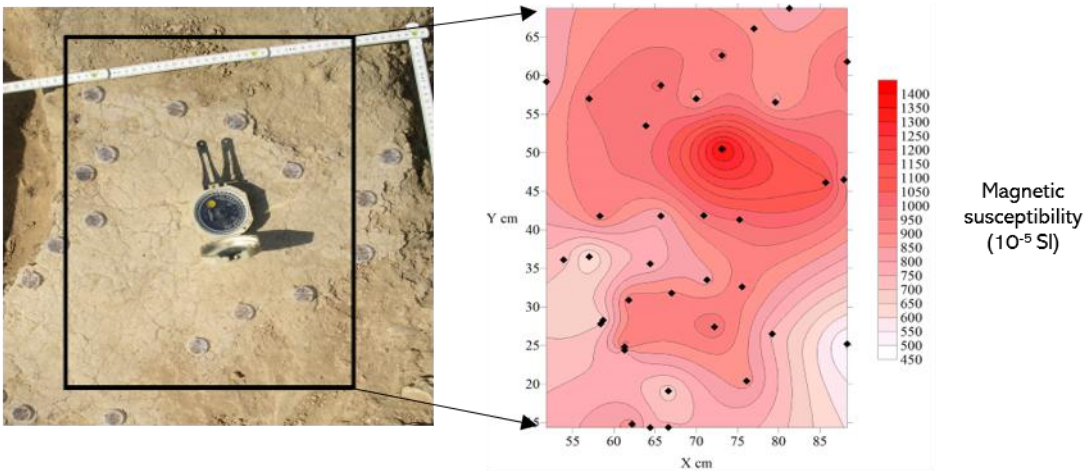
Y cm
X cm
Magnetic susceptibility (10-5 SI)

c) d)

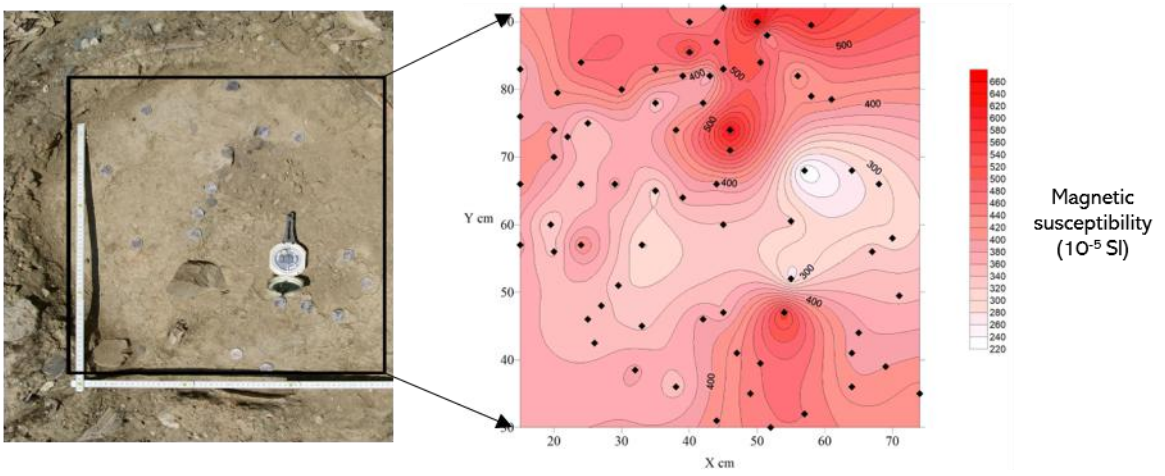
Y cm
X cm
Magnetic susceptibility (10-5 SI)

e) f)

Fig. 2

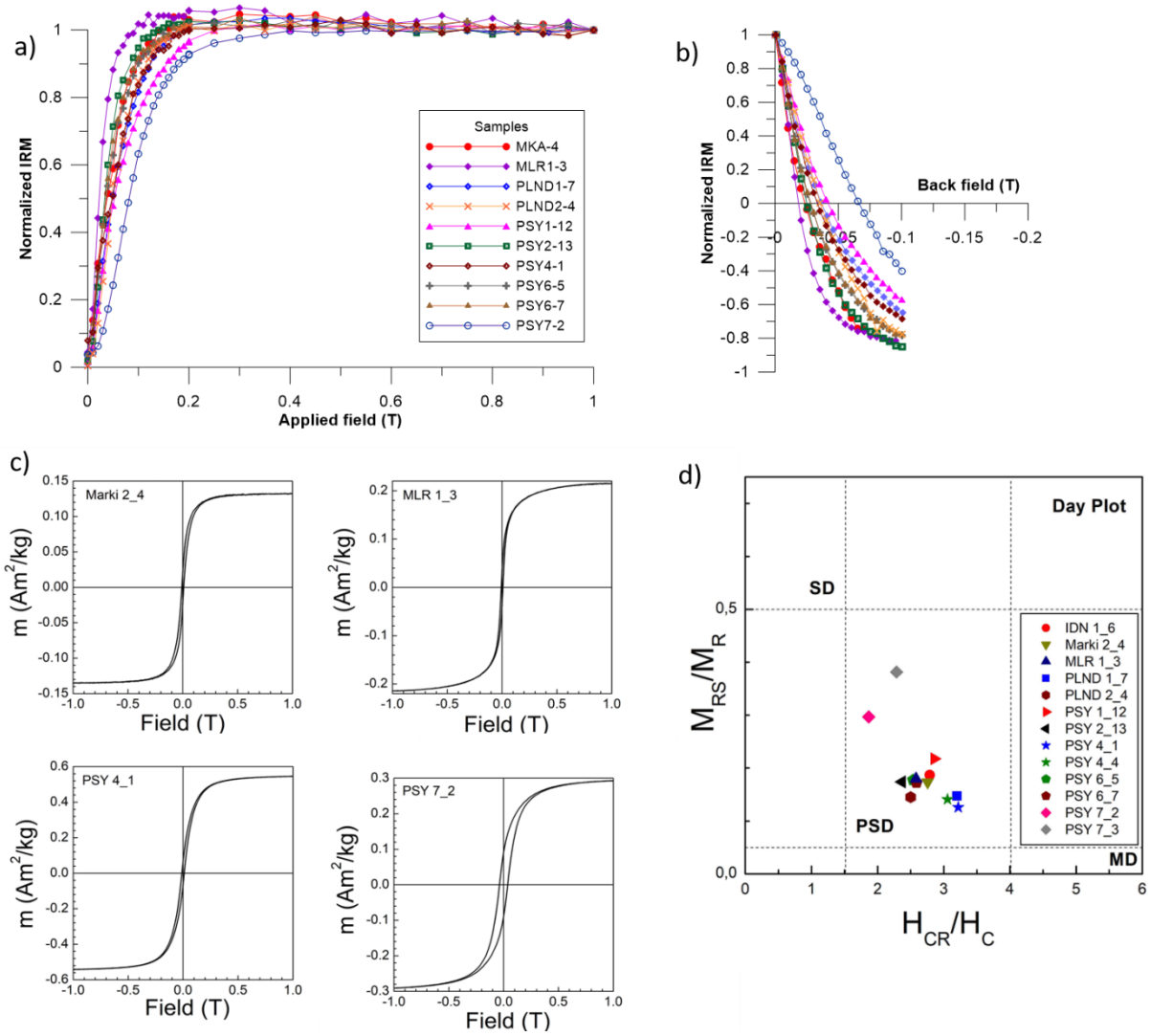
a)
Normalized IRM
Applied field (T)
Samples
MKA-4
MLR1-3
PLND1-7
PLND2-4
PSY1-12
PSY2-13
PSY4-1
PSY6-5
PSY6-7
PSY7-2
b)
Normalized IRM
Back field (T)
c)
Marki 2_4
MLR 1_3
PSY 4_1
PSY 7_2
m (Am²/kg)
Field (T)
d)
Day Plot
SD
PSD
MD
M_RS/M_R
H_CR/H_C
IDN 1_6
Marki 2_4
MLR 1_3
PLND 1_7
PLND 2_4
PSY 1_12
PSY 2_13
PSY 4_1
PSY 4_4
PSY 6_5
PSY 6_7
PSY 7_2
PSY 7_3

Fig. 3

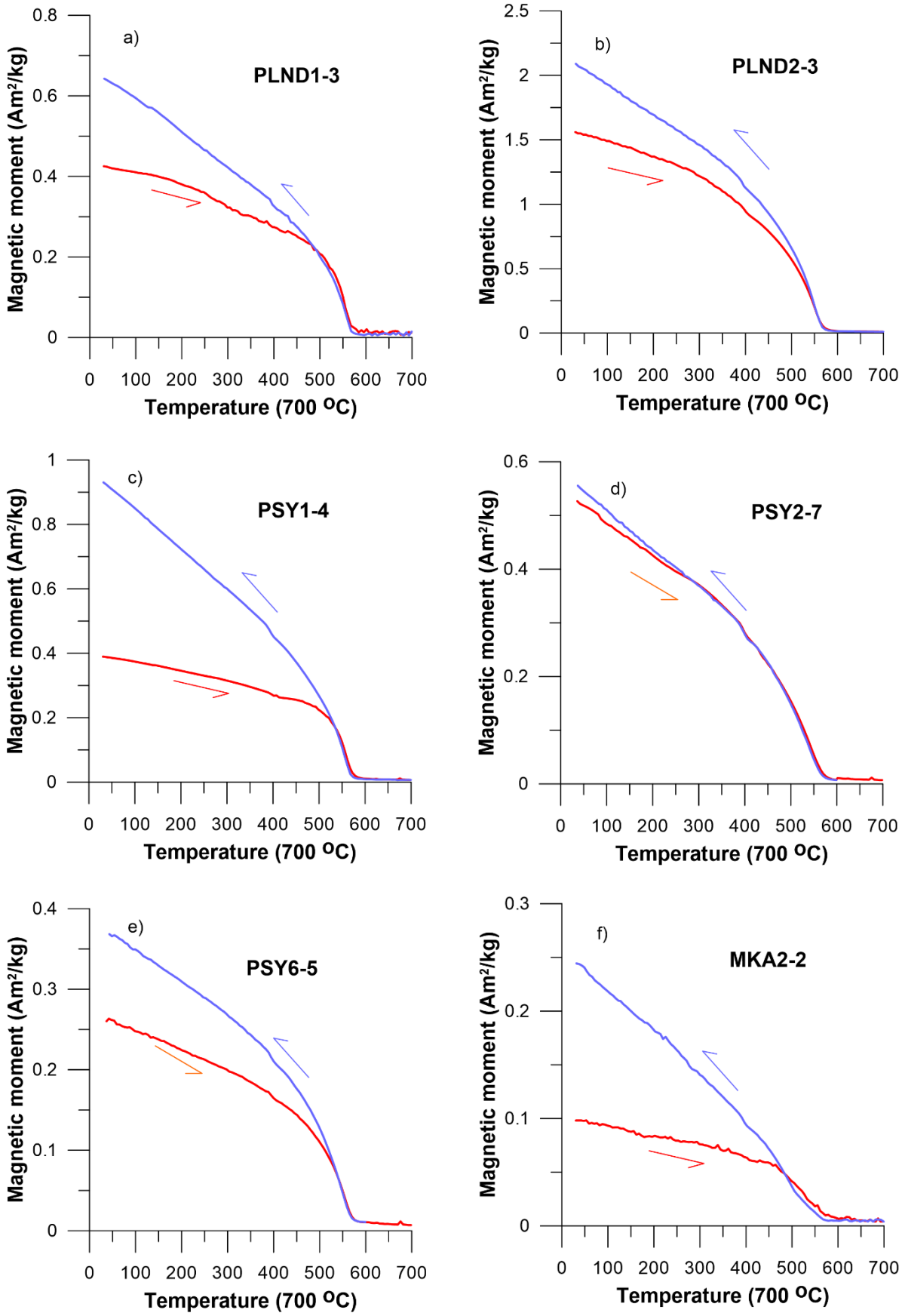

716

717

718 Fig. 4

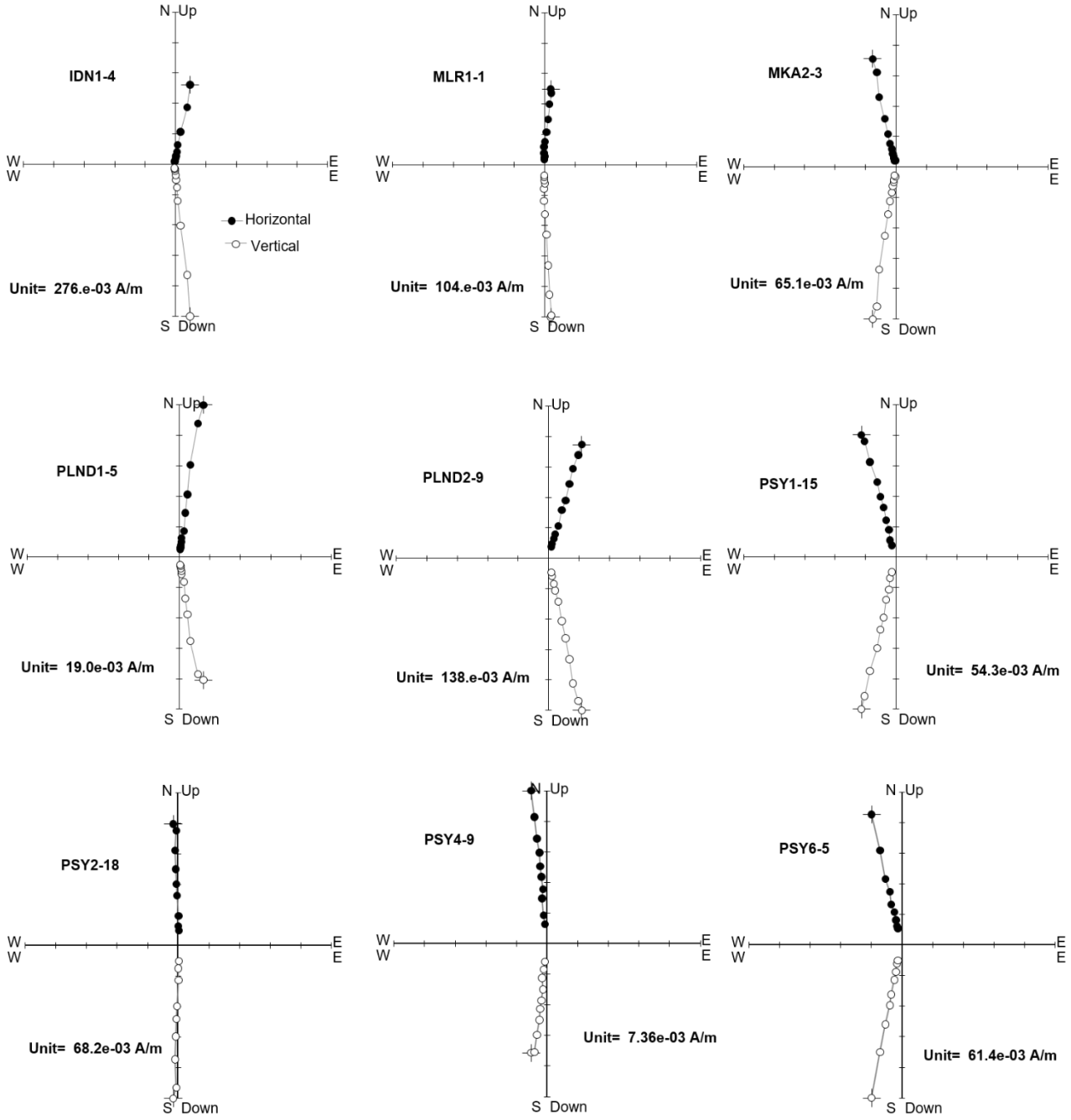

719

720

721 Fig. 5

722

723

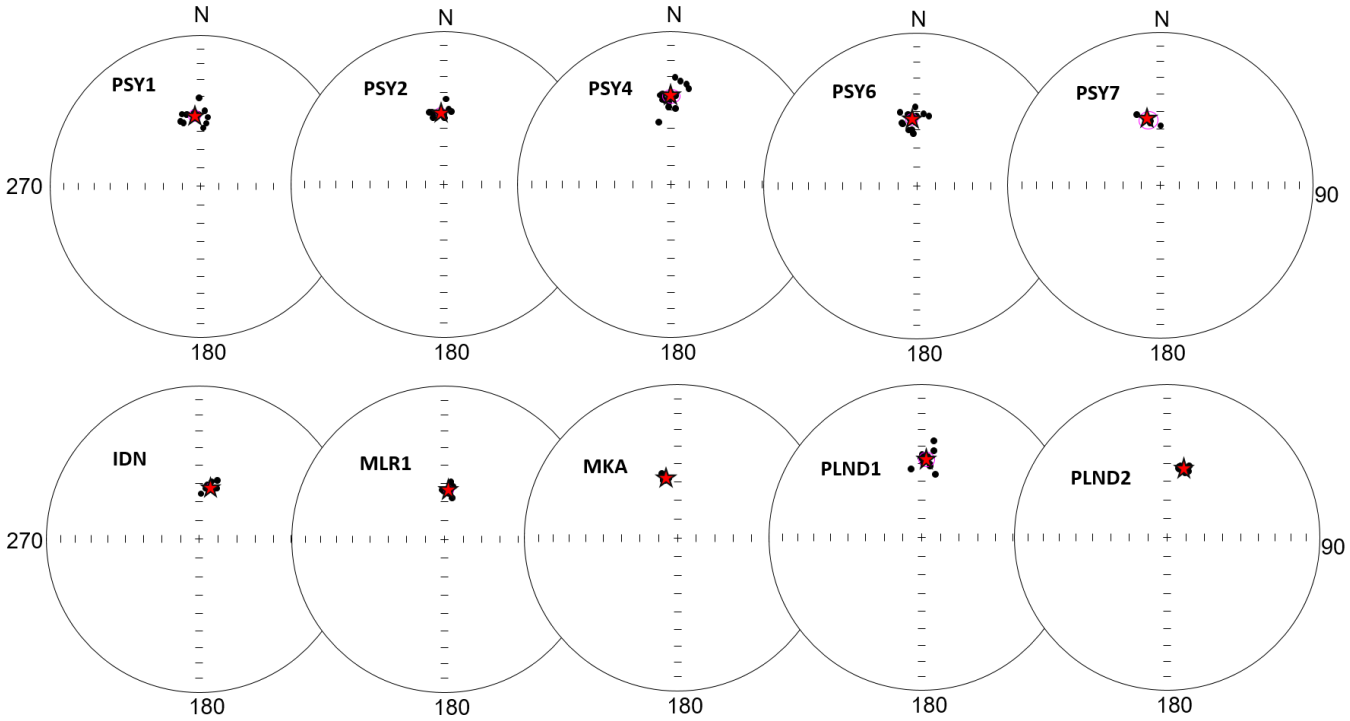

Fig. 6

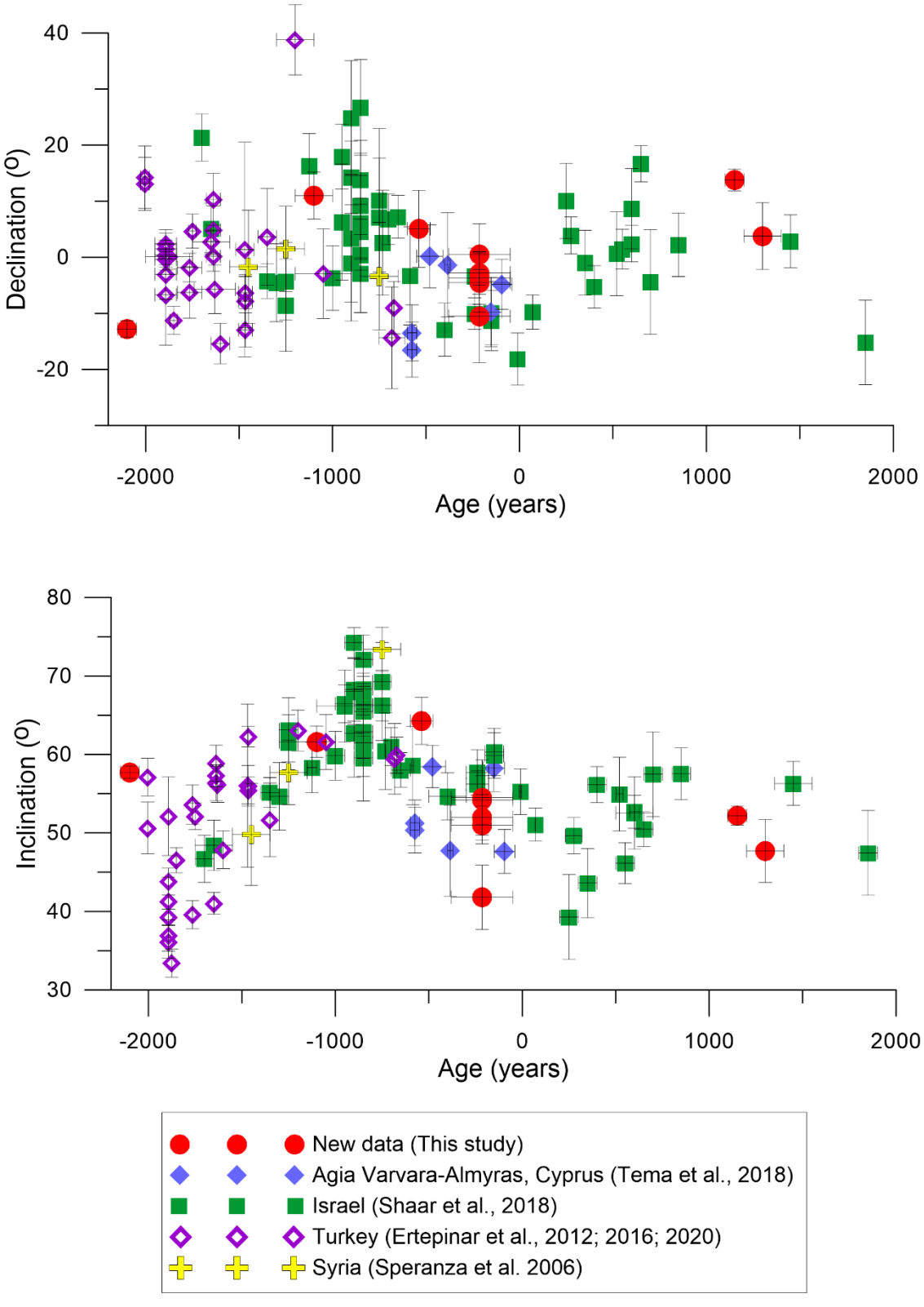

730

731 Fig. 7

732

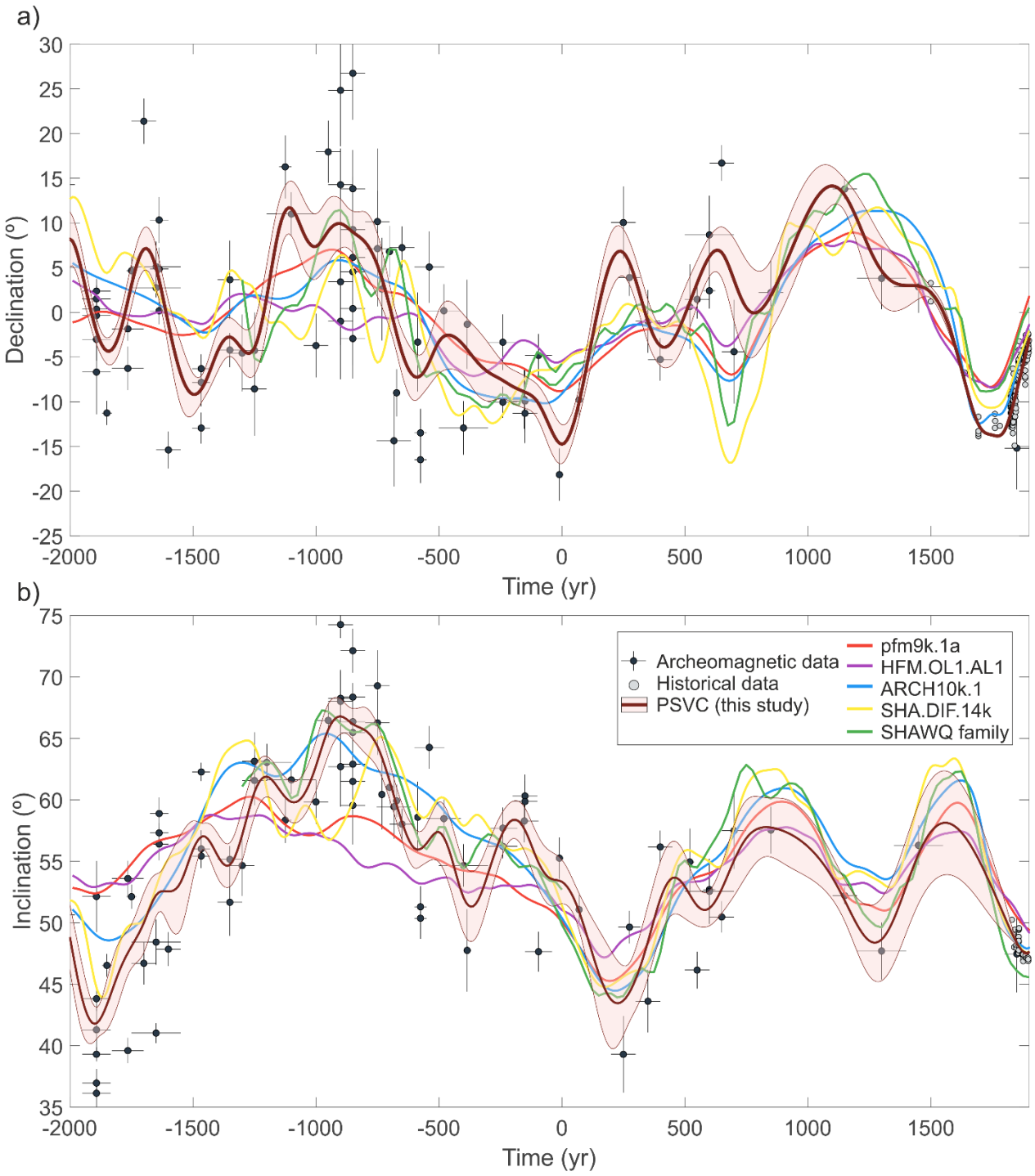
a)
Declination (°)
Time (yr)
b)
Inclination (°)
Time (yr)
Archeomagnetic data
Historical data
PSVC (this study)
pfm9k.1a
HFM.OL1.AL1
ARCH10k.1
SHA.DIF.14k
SHAWQ family

Fig. 8

738

a) Bauer diagram

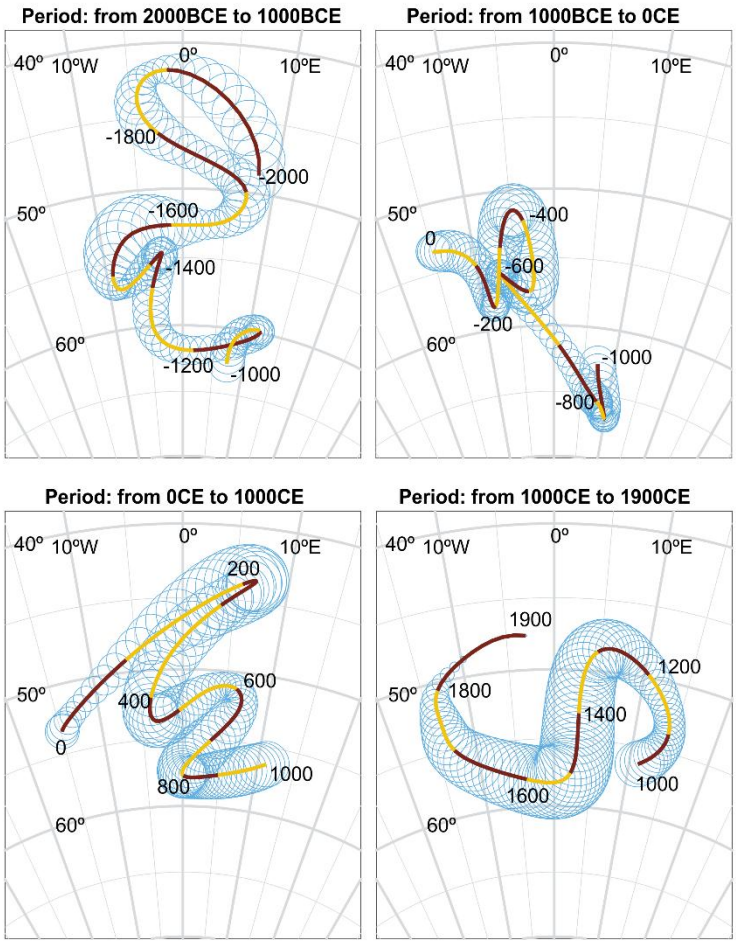

739

b) Curvature

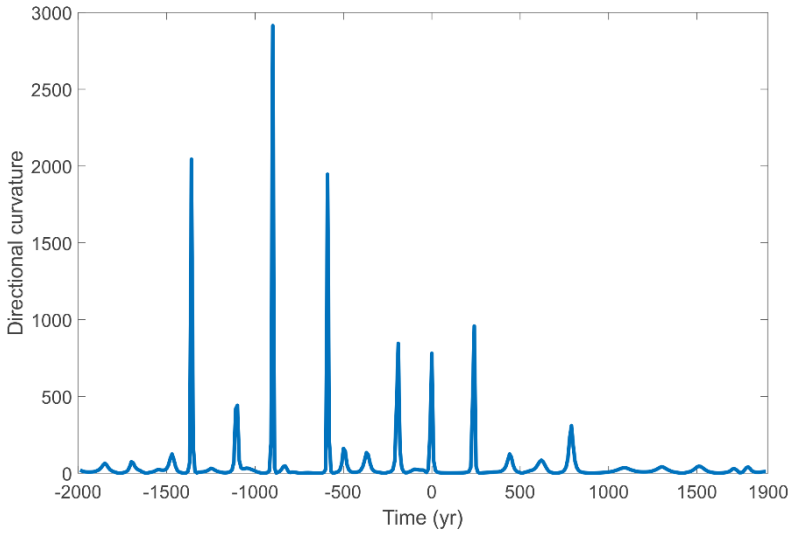

740

741

742 Fig. 9

743

Archaeological Site	Structure	Lat.	Long.	N	D (^{o})	I (^{o})	α_{95}	k	Archaeological Age
Marki	MKA (3346)	35.02^o N	33.33^o E	10	347.3	57.6	0.8	3669	2150-2050 BCE
Idalion	IDN	35.02^o N	33.42^o E	10	11.0	61.5	2.0	597	1200-1000 BCE
Athienou-Malloura	MLR2 (EU94)	35.08^o N	33.58^o E	7	5.0	64.2	3.0	401	600-480 BCE
Agios Georgios	PSY1 (13)	35.17^o N	33.35^o E	14	356.3	52.0	2.9	184	380-50 BCE
Agios Georgios	PSY2 (15a)	35.17^o N	33.35^o E	12	357.2	51.0	2.4	332	380-50 BCE
Agios Georgios	PSY4 (21)	35.17^o N	33.35^o E	14	0.5	41.8	4.1	97	380-50 BCE
Agios Georgios	PSY6 (55)	35.17^o N	33.35^o E	13	355.5	54.2	3.1	181	380-50 BCE
Agios Georgios	PSY7 (61a)	35.17^o N	33.35^o E	5	349.5	54.5	4.8	253	380-50 BCE
Palaion Demarcheion	PLND1	35.17^o N	33.37^o E	10	3.8	47.7	4.0	146	1200-1400 CE
Palaion Demarcheion	PLND2	35.17^o N	33.37^o E	13	13.8	52.2	1.2	1196	1100-1200 CE

Table 1

Supplementary material for online publication only

Click here to download Supplementary material for online publication only: Table S.1.docx

Supplementary material for online publication only

Click here to download Supplementary material for online publication only: Table S.2.docx

***Declaration of Interest Statement**

Declaration of interests

The authors declare that they have no known competing financial interests or personal relationships that could have appeared to influence the work reported in this paper.